



Suitability of chitosan nanoparticles as cryoprotectant on shelf life of restructured fish *surimi* during chilled storage

Sawssen Hajji · Marwa Hamdi · Sami Boufi · Suming Li · Moncef Nasri

Received: 13 February 2019 / Accepted: 3 June 2019 / Published online: 12 June 2019
© Springer Nature B.V. 2019

Abstract The present study investigated chitosan nanoparticle (CS-TPP NPs) preparation by ionic gelation process with chitosan (CS) and tripolyphosphate (TPP). The structural characterization of nanoparticles was studied using Dynamic Light Scattering, Nuclear Magnetic Resonance, Fourier Transform Infrared (FTIR) and X-Ray Diffraction spectroscopies. FTIR spectra confirmed that the tripolyphosphoric groups of TPP linked with ammonium groups of CS in the prepared nanoparticles. CS-TPP NPs exhibited higher antioxidant activity and an interesting antimicrobial potential. In fact, there was no report available in literature on using CS nanoparticles for the *surimi* preservation. Further, data revealed that nanoparticle incorporation in fish *surimi* effectively inhibited thiobarbituric acid substances and conjugated dienes formation, and thereby, retarding lipid oxidation. Results showed that CS-TPP NPs

were able to hinder fish *surimi* myoglobin oxidation with a significant improvement in the transformation of Heme iron. In addition, CS nanoparticles exhibited a distinguishable antimicrobial activity in the stored *surimi* during cold storage of 9 days. Thus, nanoparticles could be used as a natural ingredient to prevent lipid oxidation in *surimi* based food systems for the development of novel healthy fish products and addresses consumer demands for functional fish products.

Keywords Chitosan nanoparticle preparation · Structural characterization · Antioxidant and antimicrobial activities · *Surimi* preservation

Introduction

During the past two decades, the synthesis of nanoparticles is one of the expanding research areas in nanotechnology. With their novel properties, nanoparticles have been applied in several applications particularly medicine and other bio-related applications, such as drug delivery, photothermal therapy, wound healing and anticancer (Ruan et al. 2015; Kim et al. 2013). In addition, the nanoscale materials have been investigated for antimicrobial activity (Cioffi et al. 2005), as killing agents (Huang et al. 2003), antibiotic carriers (Gu et al. 2003) or for antitumor treatment (Bertrand et al. 2014).

S. Hajji (✉) · M. Hamdi · M. Nasri
Laboratory of Enzyme Engineering and Microbiology,
National School of Engineering of Sfax, University of
Sfax, P.B. 1173, 3038 Sfax, Tunisia
e-mail: hajjisawssen@yahoo.fr

S. Boufi
Faculty of Science of Sfax, LMSE, University of Sfax,
P.B. 802, 3038 Sfax, Tunisia

S. Li
European Institute of Membranes, UMR CNRS 5635,
University of Montpellier, Place Eugene Bataillon,
34095 Montpellier Cedex 5, France

Chitosan is a cationic polysaccharide composed of 2-acetamido-2-deoxy- β -D-glucan and 2-amino-2-deoxy- β -D-glucan units. This well-known polymer was mainly produced from chitin, present in cuticles of arthropods, the cephalopods endoskeletons and cell walls of fungi (Kaya et al. 2017). Chitosan polymer revealed very interesting physicochemical and biological properties, such as biodegradability, biocompatibility, bioactivity, high permeability, cost effectiveness and non-toxicity. Several studies have proposed CS as a biomaterial for pharmaceuticals (Kim et al. 2008), tissue engineering (Li et al. 2005a, b), cosmetics (Kim et al. 2006), food preservation (Kanatt et al. 2008) and dietary (Anraku et al. 2009), due to its antibacterial and antifungal activities (Akmaz et al. 2013) as well as immune stimulatory properties (Meshkini et al. 2012).

Chitosan-based nanoparticles were produced and used as a suitable technological platform in different applications such as gene and drug delivery. Further, different methods were studied for chitosan-based nanoparticle preparation, such as emulsion-droplet coalescence (Tokumitsu et al. 1999), emulsion solvent diffusion (Phromsopha and Baimark 2010), reverse micellization (Kafshgari et al. 2012), reverse emulsion (Divya and Jisha 2017), desolvation, or electrostatic complexation (Maciel et al. 2017). In fact, the ionic gelation appeared to be very attractive and reproducible method that produced nanometer sized particles with a narrow size distribution, as well as a highly positive surface charge. Among chemical products for nanomaterial preparation, TPP was used due to its physicochemical properties, bioactivity and environmentally friendly material and non-toxicity crosslinking-agent features, replacing glutaraldehyde or formaldehyde (Yang et al. 2010). The CS nanoparticles can be obtained by ionic gelation, when the positively charged amino groups of CS form electrostatic interactions with polyanions used as crosslinkers, such as TPP (Hosseini et al. 2015).

The CS-TPP NPs are preferably used in various applications owing to their biodegradability, biocompatibility, non-toxicity and cost effectiveness (Du et al. 2009; Arulmozhi et al. 2013). Chuah et al. (2011) and Alishahi et al. (2011) revealed that CS nanoparticles have been applied strongly in biomedical fields as agents of drug delivery, vaccine delivery and gene therapy. In addition, nanoparticles could enhance antioxidant properties and thermal stability of

encapsulated drugs and natural polyphenol (Jung et al. 2015). In fact, the most studies published to date have been focused on the chemical characteristics, such as molecular weight, acetylation degree, pH, concentration, CS to crosslinker ratio, ionic strength and the factors (temperature, rate of stirring, type of stirring, rate of addition of crosslinker). However, the CS/TPP ratio effect on biological (antioxidant and antimicrobial) activities, as well as the functional properties are often underestimated or insufficiently described. Therefore, the present study focused primarily on CS/TPP ratio effects on the physicochemical and biological properties of nanoparticles in order to their uses as an alternative to chemical food additive.

Further, to the best of our knowledge, there are no studies have been focused in the literature on using CS-TPP NPs as a conservative agent of food products. Thus, in our study, CS-TPP NPs were used in the fish *surimi* formulation due to their higher antioxidant and antimicrobial properties. Therefore, the changes in pH, weight loss, lipid oxidation, textural analysis and microbial growth of fish *surimi* during 9 days of chilled storage at 4 °C as affected by CS and CS-TPP NPs addition were performed.

Materials and methods

Materials

Chitosan (deacetylation degree of 90% and mean molecular weight of 6120 g/mol) was extracted from crab shells as previously reported (Hajji et al. 2014). Acetic acid, TPP, thiobarbituric acid (TBA) and trichloroacetic acid (TCA) were purchased from Sigma Aldrich Chemical Co., Ltd.

CS-TPP NPs preparation

CS-TPP NPs were prepared by ionic gelation method by using CS and TPP. Briefly, CS (0.5%, w/v) was dissolved in acetic acid solution (2%, v/v). CS-TPP NPs were spontaneously formed by adding 10 ml of TPP solution (0.7 mg/ml) slowly drop wise into CS solution under vigorous stirring for 30 min at room temperature (25 ± 1 °C). In our study, the effects of CS/TPP mass ratio parameter (3/1, 4/1, 5/1 and 6/1) on CS-TPP NPs properties was investigated and

nanoparticles were labeled CS-TPP NP3, CS-TPP NP4, CS-TPP NP5 and CS-TPP NP6, respectively. Subsequently, the prepared mixtures were ultrasonicated using an ultrasonic probe with diameter of 20 mm and 300 W high-intensity ultrasonic processor operating at 20 kHz for 5 min to reduce the agglomeration of nanoparticles. The resulted colloidal suspensions were centrifuged at $10,000 \times g$ for 15 min and the pellets were re-suspended in ultrapure water. Nanoparticles were washed twice to remove unreacted substances, freeze-dried and then stored at 4 ± 1 °C for further uses.

Characterizations of CS-TPP NPs

Nanoparticle recovery

The nanoparticle recovery was determined by comparing the initial weights of CS and TPP powders used for the nanoparticle preparation with the dry weights of nanoparticles suspension after centrifugation at $10,000 \times g$ for 15 min and then freeze-dried. The recovery of nanoparticles was determined using the following equation:

$$\text{Nanoparticle recovery (\%)} = \frac{\text{Weight of dried CS-TPP NPs (g)}}{\text{Weights of starting CS and TPP (g)}} \times 100$$

Structural characterization

The particle size and size distribution of CS-TPP NPs were determined by dynamic light scattering (DLS) method using Zeta sizer Nano ZS (Malvern Instrument, UK) at room temperature (25 ± 1 °C) and a scattering angle of 90°. Distilled water was used as a reference for dispersing medium.

FTIR analysis were recorded in range of 4000–400 cm^{-1} using an FTIR spectrometer (Spectrum 2000, Perkin Elmer, USA). The structural characterization and crystallinity indices of CS and CS-TPP NPs were determined by using X-ray diffractometer (D8, Advance Bruker XRD diffractometer, Germany). The X-ray powder patterns were recorded using Ni-filtered $\text{Cu-K}\alpha$ radiation of 1.54 Å, 50 kV and current of 100 mA. The samples were scanned from 2θ angles 5 to 80° at a scan speed of 0.5°/min. The crystallinity

indices (Cr I) of nanocomposite films were determined using the following formula:

$$\text{Cr I (\%)} = \frac{I_c}{I_c + I_a} \times 100$$

where: I_c and I_a are the intensities of crystalline peaks at $2\theta = 20^\circ$ and the amorphous diffraction at around 16° , respectively.

The characterization of CS and CS-TPP NPs by NMR solid-state ^{13}C and ^{31}P CP/MS spectroscopy was carried out using a Bruker W300 spectrometer with a frequency of 75.5 MHz, 50 ms acquisition time, 8 ms contact time and repetition time of 5 s.

Surface tension measurement and thermal properties of CS-TPP NPs

The surface tension of CS and CS-TPP NPs suspensions was measured according to the Du-Nouy methodology using a tensiometer TD1 (Lauda Königshofen, Germany). The thermal stability of CS-TPP NPs powders was studied using thermogravimetric analyzer (TGA Q500 High Resolution, TA Instruments), and operating under nitrogen flow. In fact, the TGA analysis was based on the mass change of samples as a function of temperature augmentation and a thermogram, showing the progressive change in mass in percentage as a function of temperature, is recorded. The CS and CS-TPP NPs samples were heated from 25 to 700 °C at a heating rate of 20 °C/min. The weight of nanoparticles samples, initially about 5 mg, was constantly measured with an accuracy of 0.01 mg.

The thermal properties of CS and CS-TPP NPs were further studied by using Differential Scanning Calorimeter (DSC, Modulated DSC Q20, TA Instruments) equipped with a liquid nitrogen cooling system. The DSC was used to estimate the melting and crystallization points, as well as the glass transition of the prepared nanoparticles. CS-TPP NPs samples were accurately weighed into sealed aluminum pans. An empty capsule serves as an inert reference and the apparatus was calibrated using indium. The thermal profile of samples was analyzed in a temperature range of 0–200 °C at a heating rate scan of 10 °C/min and under a nitrogen flow rate of 50 ml/min. Thermograms were then analyzed by using TA Universal V4.5A software.

Solubility of CS-TPP NPs

The solubility of CS-TPP NPs was determined according to the method of Fernandez-Kim (2004). CS and CS-TPP NPs powders (0.1 g) were placed into a pre-weighed centrifuge tube, and then dissolved in 10 ml acetic acid (1%) for 30 min at 25 ± 1 °C, under constant stirring. The solutions were then heated in a boiling water bath for 10 min. After cooling at room temperature (25 °C), centrifugation was carried out at $8000 \times g$ for 10 min, and the supernatant was decanted. The pellet was dissolved in distilled water (25 ml) and then centrifuged at $8000 \times g$. The supernatant was discarded and undissolved pellet was dried at 50 ± 1 °C for 24 h. The solubility was determined as follow:

$$\text{Solubility (\%)} = \frac{W_1 - W_2}{W_1 - W_0} \times 100$$

where W_1 and W_2 are the initial weight of (tube + sample) and the final weight of (tube + sample), respectively, and W_0 is initial mass of tube.

Antioxidant activity of CS-TPP NPs

2,2-Diphenyl-1-picrylhydrazyl (DPPH) free radical-scavenging activity

DPPH free radical-scavenging activity of CS-TPP NPs was determined according to the method described by Yen and Wu (1999). A volume of 500 μ l of each sample at different concentrations was added to 375 μ l of ethanol and 125 μ l of DPPH (0.2 mM) dissolved in ethanol (99.50%) and mixed thoroughly. After that, the mixture was kept for 60 min in dark at room temperature (25 ± 1 °C) and the absorbance was measured at 517 nm. The lower absorbance of the reaction mixture indicated a higher free radical-scavenging activity. DPPH radical-scavenging activity was calculated as follow:

$$\text{DPPH radical - scavenging activity (\%)} = \frac{A_{\text{Control}} - A_{\text{Sample}}}{A_{\text{Control}}} \times 100$$

where A_{control} and A_{sample} are the absorbances of control and sample reactions, respectively. BHA was used as a positive control. The analysis was carried out in triplicate.

Ferric reducing power assay

The ability of the prepared CS-TPP NPs to reduce iron (III) was determined as described by Yildirim et al. (2001). An aliquot of 0.5 ml of each nanoparticles sample was mixed with 1.25 ml of phosphate buffer (0.2 M, pH 6.6) and 1.25 ml of potassium ferricyanide (1%, w/v). The mixture was incubated at 50 ± 1 °C for 30 min and the reaction was stopped by addition of 1.25 ml of TCA (10%, w/v). Finally, 1.25 ml solution from the mixture was mixed with 1.25 ml of distilled water and 250 μ l of ferric chloride (0.1%, w/v) solution. The mixture was incubated at room temperature (25 ± 1 °C) for 10 min and the absorbance was measured at 700 nm. BHA was used as a positive control.

β -carotene bleaching method

The capacity of CS-TPP NPs to prevent the bleaching of β -carotene was performed as described by Koleva et al. (2002). Thus, 0.5 mg of β -carotene was dissolved in 25 μ l of linoleic acid, 200 μ l of Tween-80 and 1 ml of chloroform. The mixture was completely evaporated under vacuum in a rotary evaporator at 50 °C. Thereafter, 100 ml of bi-distilled water was added, and the resulting solution mixture was vigorously stirred. A volume of 2.5 ml of the β -carotene/linoleic acid-emulsion was transferred to test tubes containing 0.5 ml of each sample. Following incubation for 1 h at 50 ± 1 °C, the absorbance was measured at 470 nm. A control reaction was consisted of 0.5 ml of distilled water instead of the sample. The same procedure was performed with BHA as a positive control. The β -carotene bleaching inhibition was calculated using the following equation:

$$\beta\text{-carotene bleaching inhibition (\%)} = 1 - \left[\frac{(A_0 - A_t)}{A'_0 - A'_t} \right] \times 100$$

where A_0 and A'_0 are the absorbances, measured at time 0, of sample and control, respectively. A_t and A'_t are the absorbances, measured after 1 h, of sample and control, respectively. Tests were carried out in triplicate.

2,2'-azinobis(3-ethylbenzothiazoline-6-sulfonic acid) (ABTS) radical-scavenging activity

The ABTS radical-scavenging activity of the prepared nanoparticles was determined as described by Wang et al. (2012) with slight modification. A volume of 1 ml of diluted ABTS solution was mixed with 1 ml of each CS-TPP NPs sample solution at various concentrations (1–5 mg/ml). The mixture was left at room temperature (25 ± 1 °C) in the dark. The absorbance was measured at 734 nm using a spectrophotometer against the corresponding control. The control was prepared in the same manner, except that distilled water was used instead of the sample. The ABTS scavenging activity of samples was calculated as follow:

$$\text{ABTS - scavenging activity (\%)} = \frac{(A_{\text{Control}} - A_{\text{Sample}})}{A_{\text{Control}}} \times 100$$

where A_{control} and A_{sample} are the absorbances of control and sample reactions, respectively.

Antimicrobial tests

The antibacterial activities of CS-TPP NPs solutions (10 mg/ml) were investigated against *Bacillus cereus* (ATCC 11778), *Staphylococcus aureus* (ATCC 25923), *Micrococcus luteus* (ATCC 4698), *Salmonella enterica*, *Escherichia coli* (ATCC 25922), *Enterobacter*, *Salmonella typhimurium*, *Klebsiella pneumoniae* (ATCC 13883) and *Pseudomonas aeruginosa* (ATCC 27853) bacteria using agar disc method. The antifungal activity was tested against *Fusarium solani* and *Rhizoctonia solani* strains. The culture suspension (100 µl) of each tested microorganism (10^6 CFU/ml for bacteria and 10^8 spores/ml for fungal strains) were spread over the Luria–Bertani agar and Potato Dextrose Agar medium, respectively. After that, 60 µl of each CS-TPP NPs solution was delivered into wells (5-mm depth, 5-mm diameter) previously cut in the agar. The antagonistic zones were detected after incubation at 37 ± 1 °C for 24 h for bacteria and 72 h at 30 ± 1 °C for fungal strains. Antimicrobial activity was evaluated by measuring the diameter of growth inhibition zones in millimeters (including well diameter of 5 mm).

Water and fat-binding capacities

The water and fat-binding capacities (WBC, FBC) of CS and CS-TPP NPs were determined as referred to Ocloo et al. (2011). Briefly, 0.5 g of sample was placed in a pre-weighed centrifuge tube and 10 ml of distilled water (or corn oil) were added. CS-TPP NPs were then suspended by means of a vortex mixer for 1 min, before left at ambient temperature (25 ± 1 °C) for 30 min, with intermittent shaking for 5 s every 10 min. After being centrifuged at $5000 \times g$ for 25 min, the supernatants water or oil were decanted and the tube was weighed again. Tests were carried out in triplicate. WBC or FBC were calculated using the following equation:

$$\text{Binding capacity (g/g sample)} = \frac{\text{Water (or oil) bound (g)}}{\text{Initial sample weight (g)}}$$

Surimi preservation using CS-TPP NPs

Fish samples

Frigate grey mullet fishes with an average weight of 80–100 g were purchased caught from local supermarket in Sfax, Tunisia. The fish, off-loaded approximately 12 h after capture, was placed in ice with a fish/ice ratio of 1:2 (w/w) and transported to the laboratory within 20 min. Fish were immediately washed, gutted, filleted, skinned and the whole muscles were collected. To prepare fish mince, fish fillets were minced to uniformity using a meat grinder. The muscles were kept on ice during preparation.

Surimi preparation

To prepare *surimi* by conventional washing process, fish mince was washed with cold water (4 ± 1 °C) using a water/mince ratio of 3:1 (v/w). The mixture was stirred gently for 10 min in a cold room (4 ± 1 °C) and the washed mince was filtered with a layer of nylon screen. Washing was performed three times. Finally, the washed mince was pressed and was referred to as '*surimi*'. The *surimi* was subdivided on three groups as follow: **Control lot:** *Surimi* sample

without any supplementation; **Chitosan lot (CS)**: *Surimi* sample supplemented with CS (1%, g/g of *surimi*) and **CS-TPP NPs lot**: *Surimi* sample supplemented with CS-TPP NPs (1%, g/g of *surimi*). The *surimi* samples were cooked at 90 °C for 20 min, cooled at room temperature (25 ± 1 °C) and then stored at 4 ± 1 °C until uses. Groups were sampled at 1, 3, 6 and 9 days of storage for physicochemical characteristics and microbial analyses.

Moisture, weight loss and pH measurements of *surimi*

Moisture content in *surimi* samples was determined in triplicate by the oven drying method at 105 ± 1 °C until constant weight. The pH values of *surimi* from each treatment were measured. Thus, 10 g of the sample was homogenized with 50 ml of distilled water for 2 min using an Ultra-Turrax apparatus (IKA T18 Basic, Germany). The sample was transferred into a beaker and pH was determined using a combined glass electrode pH meter (Metrohm AG pH lab system, France) by directly immersing the electrode into the homogenates.

Weight loss (WL) of *surimi* samples was monitored during the storage using an analytical balance by weight determination at 1, 3, 6 and 9 days (W_i), as compared to their initial weight (W_0) and expressed as follow:

$$WL (\%) = \frac{(W_0 - W_i)}{W_0} \times 100$$

where W_0 and W_i are the initial and final weights of samples, respectively.

Myoglobin content determination

The myoglobin content in *surimi* was determined by direct spectrophotometry measurement as described by Benjakul and Bauer (2001). An aliquot of 2 g of each sample was weighed into a 50 ml polypropylene centrifuge tube and 20 ml of cold phosphate buffer (40 mM, pH 6.8) was added. The mixture was homogenized at 13,500 rpm for 10 s, followed by centrifugation at 3000 × *g* for 30 min at 4 ± 1 °C. The supernatant was filtered with Whatman No. 1 filter paper. The myoglobin content was determined at 555 nm, and calculated from the millimolar extinction coefficient of 7.6 and molecular weight of 16,400 (Gomez-Basauri and Regenstein 1992). The myoglobin content was expressed as mg/g of sample.

Metmyoglobin determination

The oxidation of myoglobin of *surimi* samples from different groups was determined spectrophotometrically. Metmyoglobin determination was performed as described by Hansen and Sereika (1969). The ratio of A_{630}/A_{525} was calculated. In fact, a high A_{630}/A_{525} ratio indicates a high relative proportion of metmyoglobin.

Lipid peroxidation assessment

Oxidative rancidity of *surimi* samples was measured by a TBARS assay of malondialdehyde (MDA). The absorbance was measured at 535 nm using an UV-Vis spectrophotometer. The TBARS values were calculated using molar absorption of MDA (156,000 M/cm) at 535 nm. The TBARS values were reported as mean values (± standard deviation) of at least three replicates and the mean values were expressed as µg of MDA per g of *surimi* sample.

Lipid oxidation was likewise evaluated by the conjugated dienes content and measured at 233 nm (Esterbauer et al. 1982).

Texture profile analysis

Texture profile analysis of *surimi* was performed using a TA-XT2i texture analyzer (Stable Micro Systems, Godalming, Surrey, UK). Samples were subjected to two-cycle compression at 50% compression using the texture analyzer with a 1-cm TPA compression plate attachment moving at a speed of 10 mm/min. From the resulting force–time curves, hardness, cohesiveness ratio, springiness, chewiness and adhesiveness were evaluated using the texture analyzer. Hardness was measured with a probe during the first compression. Cohesiveness ratio was the measure of the area of work during the second compression divided by the area of work during the first compression. Springiness was calculated as the force at maximum compression during the second compression cycle. Chewiness was determined as the product of gumminess and springiness by measuring the energy required to chew a solid sample to a steady state of swallowing. Finally, the adhesiveness was defined as the negative force area under the curve obtained between cycles.

Microbiological analysis

In order to determine the bacteriological counts in the preserved *surimi*, 1 g portion of sample from each group was aseptically transferred into sterile tube and then homogenized with 9 ml of sterile saline solution (0.9%, w/v). From this solution, tenfold serial dilution of *surimi* homogenates were prepared and used for bacterial and fungal enumeration. Total psychrotrophic and mesophilic bacteria were determined by the pour plate technique using plate count agar and incubated for 24–72 h at 4 ± 1 °C and 37 ± 1 °C, respectively. Yeast and molds counts were performed using surface seeding technique with potato dextrose agar for 3–5 days at 30 ± 1 °C. All microbial counts were expressed as logarithms of colony-forming units per gram of *surimi* (log CFU/g).

Statistical data analysis

All experiments were carried out in triplicate, and the average values with standard deviation errors were reported. Mean separation and significance were analyzed via the SPSS software package ver. 13.0 professional edition (SPSS, Inc., Chicago, IL, USA), using ANOVA analysis based on Duncan's multiple range test to estimate the significance among the main effects at the 5% probability level.

Results and discussion

Synthesis and characterization of CS-TPP NPs

CS/TPP mass ratio is critical to control the particle size and size distribution. Different CS/TPP mass ratios (3/1, 4/1, 5/1 and 6/1) were prepared using a constant CS concentration (0.5 mg/ml) and the average hydrodynamic particles size of CS-TPP NPs was analyzed by DLS (Fig. 1A). A strong dependence of the particle size and size distribution could be observed according to the ratio CS/TPP (Table 1). The highest particle size for the prepared CS-TPP NPs was attained for CS/TPP ratio of 3/1 (321.5 nm) (CS-TPP NP3) and steadily decreased as the ratio CS/TPP is going up, reaching 121.6 nm for CS-TPP NP6. This effect could be explained by the increase in the crosslinking density as the ratio CS-TPP is getting higher. Indeed, with higher concentration in CS in the

solution, more positive charges will be available to interact ionically with the negative charges of multi-valent TPP, giving rise to a dense crosslinked network. The higher crosslinking density to more compact will be the network that will segregate in tiny nanoparticles under the effect of sonication.

Chitosan nanoparticles were formed spontaneously due to the interaction between the negatively charged groups of TPP and the positively charged amino groups of CS, as reported earlier (Calvo et al. 1997). Further, TPP addition on CS solution leads to ionic gelation and thus nanoparticle formation. Dudhani and Kosaraju (2010) reported that size distribution of CS-TPP NPs was ranged from 20 to 600 nm. However, Nguyen et al. (2017) showed that the mean size of CS nanoparticles was in range of 166–1230 nm, depending on the molecular weight of CS and size of the spray dryer nozzles. In addition, results showed that the prepared CS-TPP NPs were characterized by a high recovery percent in the range of 100–201% (Table 1), depending on the CS/TPP ratio used for the CS-TPP NPs preparation.

It was shown that CS had a surface activity at concentration of 0.5 mg/ml about 46.1 mN/m, which is in agreement with data reported by Calero et al. (2010). The surface activity was explained by the formation of CS monolayer at the air–water interface, hiding water molecules from the surface.

The surface (water–air) tension of CS-TPP NPs solutions has been studied. Results showed an increase in the interfacial tension for the NPs with the increase of CS/TPP ratio mass. This effect is likely due to the consumption of CS from the solution, leaving a small fraction of CS available at the air–water interface. This result also is indicative of a lack of surface activity of CS-TPP NPs, presumably due the impossibility of adsorb at water–air interface.

FTIR analysis

FTIR spectroscopy was used in order to confirm the linkage between phosphoric and ammonium ions of TPP and CS in the prepared nanoparticles (Fig. 1B). In the CS spectra, the characteristic peaks were observed at 3365 cm^{-1} (–OH and –NH₂ stretching), 2870 cm^{-1} (–CH stretching), 1660 cm^{-1} (amide I) and 1075 cm^{-1} (C–O–C asymmetric stretching). The sharp peaks at 1371 cm^{-1} and 1427 cm^{-1} can be assigned to the –CH₃ symmetrical stretching band

Fig. 1 Structural characterization of CS-TPP NPs as compared to CS by DLS (A), FTIR (B) and XRD (C) spectroscopies

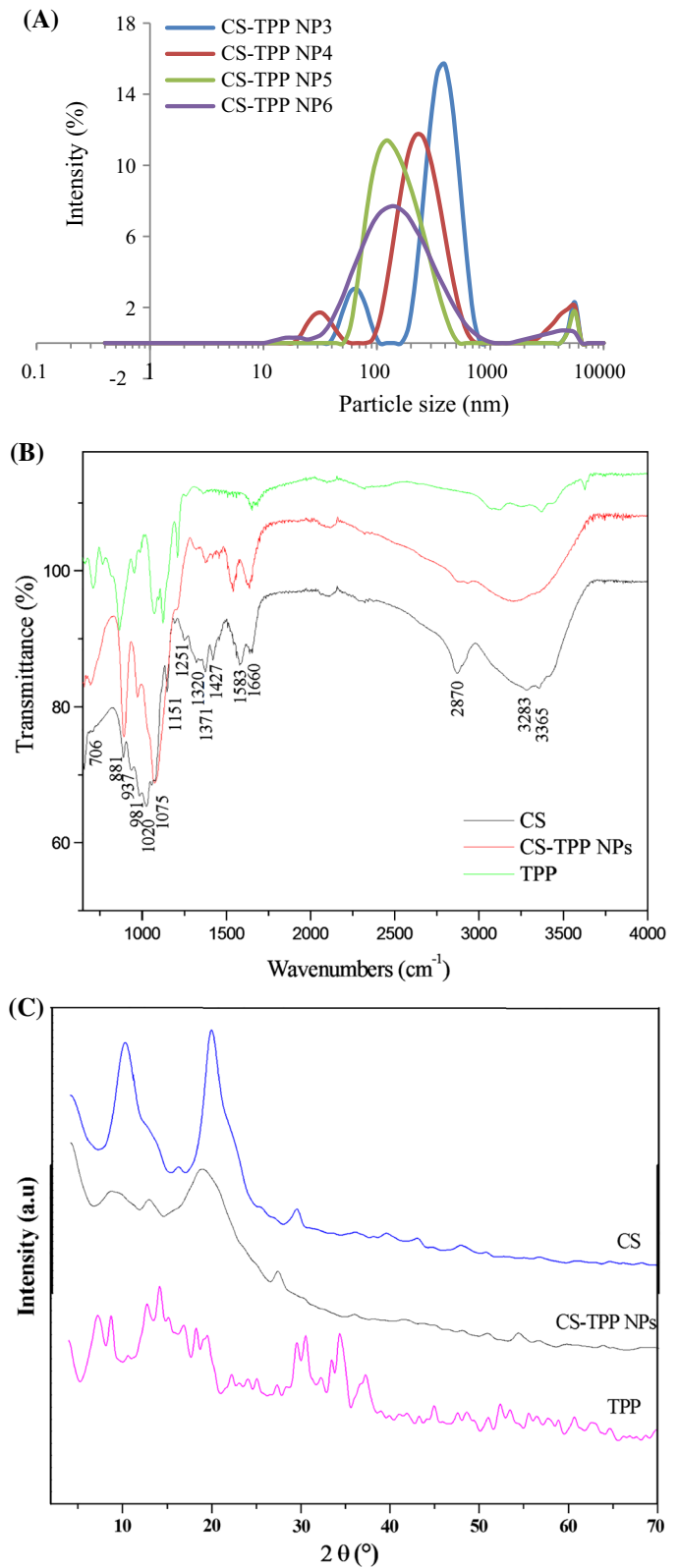


Table 1 Determination of nanoparticles size, surface tension and recovery percent of the prepared CS-TPP NPs, as compared to CS polymer

Samples	Nanoparticles size (nm)	Surface tension (mN/m)	Recovery percent (%)
CS	606.5 ± 0.25 ^a	46.1 ± 0.1 ^c	–
CS-TPP NP3	321.50 ± 0.54 ^b	52.80 ± 0.30 ^d	103 ± 2.30 ^d
CS-TPP NP4	201.20 ± 0.15 ^c	53 ± 0.25 ^c	100 ± 0.14 ^c
CS-TPP NP5	153.90 ± 0.10 ^d	58.20 ± 0.09 ^b	178 ± 2.45 ^b
CS-TPP NP6	121.60 ± 0.40 ^c	59.30 ± 0.10 ^a	201 ± 0.67 ^a

Means with different superscripts (a–e) within a column indicate significant difference ($p < 0.05$)

(Dudhani and Kosaraju 2010). For the band at 1060 cm^{-1} , it was assigned to the second –OH group of CS polymer. For FTIR spectrum of TPP powder, two intense absorption peaks observed at 1210 cm^{-1} and 860 cm^{-1} were assigned to P=O stretching and P–O along with P–O–P (Rodrigues et al. 2012).

By comparing FTIR spectra of CS-TPP NPs and CS, several changes were observed. The bands corresponding to the O–H and N–H stretching vibrations (3334 and 2884 cm^{-1} , respectively) were broader indicating the involvement of –OH and –NH groups in the crosslinking process, presumably through hydrogen bonding within CS-TPP network. In addition, the C=O and –NH₂ vibrations bands (1660 and 1583 cm^{-1}) shifted to lower wavenumber (1635 and 1547 cm^{-1}), which clearly confirms the electrostatic interaction between NH₃⁺ groups of CS and the polyphosphoric groups of TPP (Dudhani and Kosaraju 2010; Jingou et al. 2011). Moreover, the band observed at 1251 cm^{-1} strongly weakened in intensity or even vanished with emergence of a new peak around 1218 cm^{-1} (C–O–C stretching). The bands at 1203 and 895 cm^{-1} in the CS-TPP NPs spectra were attributed respectively to P=O stretching vibration and P–O–P asymmetric stretching vibration, confirming the presence of P–O–P linkage within CS-TPP NPs. The bending vibration in C–H groups of acetyl (1371 cm^{-1}) shifted to 1380 cm^{-1} for the CS-TPP NPs. At 1070 and 690 cm^{-1} , the peaks were assigned to stretching of C–O–C and stretching of the pyranoside ring (Hebeish et al. 2013). The shifts and the changes in the vibration frequencies in this particular region is due to electrostatic interaction between amino groups of CS and polyphosphoric groups of TPP (de Pinho Neves et al. 2014).

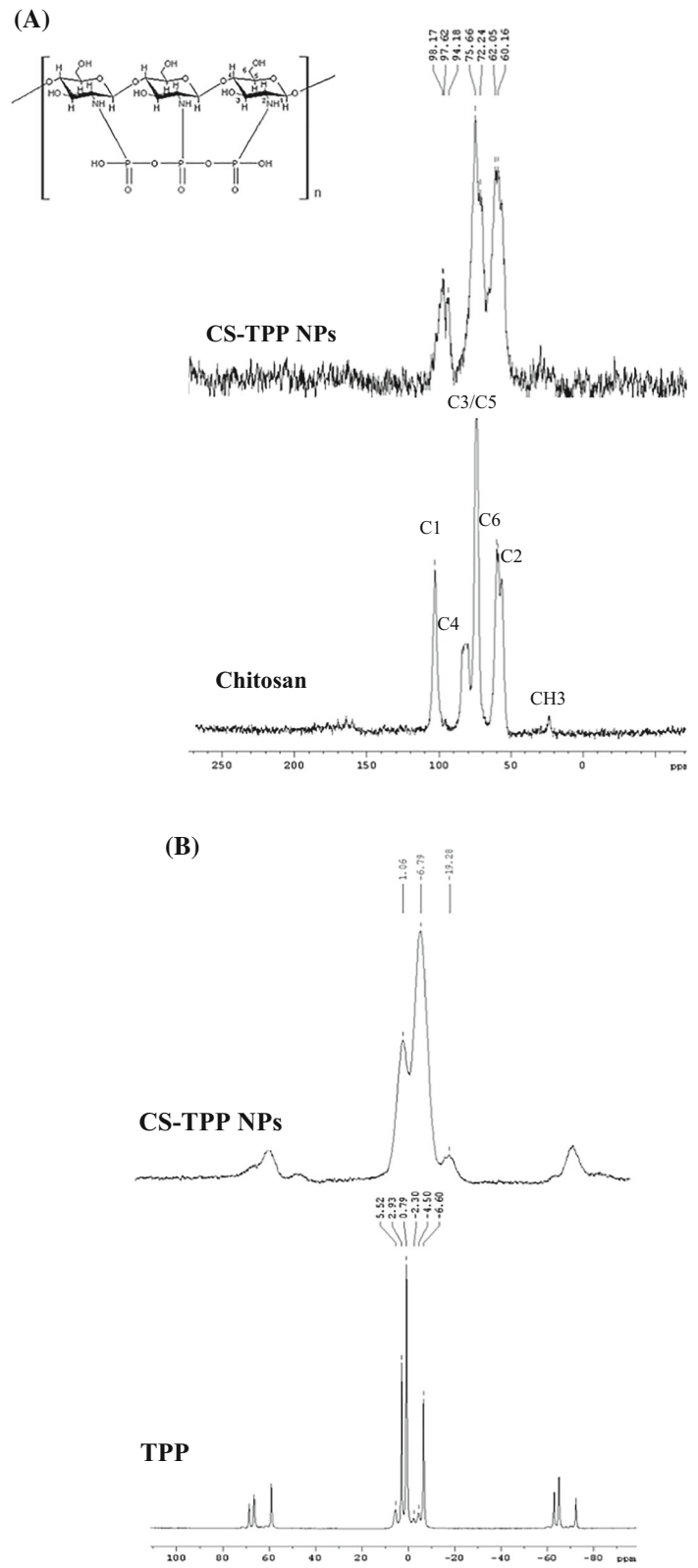
X-ray diffraction

The XRD analysis was carried out to determine the crystallinity of the materials. Pure CS shows diffraction peaks at $2\theta = 10.05^\circ$ and 19.86° (Fig. 1C) corresponding to the respective equatorial (020) and (110) of the microcrystalline reflections of CS (Jingou et al. 2011). After ionic cross-linking with TPP, the diffraction peaks were observed at 12.85 , 18.83 and 27.26° , with substantially lower intensity, indicating that CS-TPP NPs are more amorphous than CS polymer, with almost no ordered structure (Jingou et al. 2011). This effect is expected if we consider that the crosslinking reaction reduces the possibility long range order within the CS-TPP network (Rokhade et al. 2006). The crystallinity indices of CS and CS-TPP NPs were 51.18% and 35.03% , respectively. Similar results were reported by León et al. (2017) for CS-TPP NPs dried with supercritical CO₂.

¹³C and ³¹P NMR characterization

¹³C CP/MAS NMR spectra of CS and CS-TPP NPs are depicted in Fig. 2A. CS spectrum was characterized by the presence of five bands at 57.85 , 60.08 , 75.63 , 83.31 and 105.31 ppm, that correspond to the pyranose rings carbon atoms (C2, C6, C3/C5, C4 and C1; respectively). Additionally, the methyl and carbonyl carbons of the acetyl group of N-acetyl-glucosamine units in CS (at 21 and 175 ppm, respectively) were reduced due to the deacetylation process. As compared to CS, CS-TPP NPs spectra showed similar peaks but broader and with lower resolution, which could be related to the layout of CS chains and TPP molecules forming an amorphous structure of CS-TPP NPs.

Fig. 2 ^{13}C NMR spectra of CS and CS-TPP NPs (A) and ^{31}P NMR spectra of CS-TPP NPs and TPP powder (B)



The ^{31}P NMR spectra of CS-TPP NPs, as compared to TPP powder, were shown in Fig. 2B. As observed, the NMR spectra of the commercial TPP powder, used in the nanoparticle preparation, showed several peaks in the region between -7 and 6 ppm, indicating that its powder represents a mixture of two crystalline phase polymorphs of $\text{Na}_5\text{P}_3\text{O}_{10}$ and $\text{Na}_5\text{P}_3\text{O}_{10}\cdot 6\text{H}_2\text{O}$. Further, the ^{31}P spectra of CS-TPP NPs showed a broad peak, characteristic of amorphous materials, suggesting the amorphous structure of phosphate groups in the prepared NPs. At -6.79 ppm, it was observed a broad and asymmetric peak, which could be attributed to the terminal phosphate units in the amorphous TPP, and a small peak at -19.28 ppm, characteristic of phosphate linked by two phosphate units $(\text{PO}_{4/2})^{3+}$, suggesting the presence of interaction between CS and TPP in the CS-TPP NPs, that was achieved by the pyrophosphate units and few interactions by TPP (Vasconcelos et al. 2008). These results are in line with those cited by Barbi et al. (2015), who reported the same peaks and shifting to -4.2 and -17.3 ppm.

Thermal gravimetric analysis

TGA is a useful analytical analysis to determinate the weight loss of the prepared CS-TPP NPs as a function of temperature or time. The decomposition Temperature (T_d) is the temperature corresponding to the maximum slopes of each weight change step. The T_d is obviously seen as a peak when the rate of mass loss with respect to temperature in Derivative Thermo Gravimetry (DTG) thermograms. The TGA curves profiles revealed the decrease in weight of CS and CS-TPP NPs with increasing in the temperature from 30 to 600 °C (Fig. 3A). The CS is characterized by two major phases. The initial weight loss of about 6% around 100 °C in neat CS is due to moisture evaporation (Table 2). In CS-TPP NPs, the second weight loss of about 10% around 150 °C is observed which is due to removal of water entrapped within the CS-TPP network (dehydration). The shift of water evaporation to higher temperature is presumably due to the strong interaction of water molecules with CS-TPP network, presumably through strong hydrogen bonding. A third weight loss is observed around 300 °C is due to the thermal degradation of the D-glucosamine units of CS

polymer. The residual mass of CS was at about 17.50% at 600 °C, corresponding to ash content composed of mineral residue of CS-TPP.

The thermal decomposition T_d of CS-TPP NPs clearly observed in Fig. 3B was ranged from 294 to 298 °C (Table 2), which was lower than that of CS polymer (329.47%). Consequently, it can be deduced that CS and CS-TPP NPs were decomposed at a higher temperature, reflecting their improved thermal stability. Moreover, the total weight loss of CS-TPP NPs was nearly 37.51 , 45.51 , 42.45 and 32.48% for CS-TPP NPs 3, 4, 5 and 6, respectively. Thus, it could be concluded that thermal stability was correlated with the composition of CS-TPP NPs and especially the CS/TPP mass ratio. In fact, the use of TPP for the CS-TPP NPs preparation induced a modification in the crystalline nature of CS polymer, thus making the two molecules more stable on heating, which have also reported a good stability of CS-NPs.

The degradation profile of CS-NPs seems to be different compared to CS, but stable than CS which proves that the system is amorphous nature. When compared with CS-TPP NPs, the residual mass is higher than CS (17%). This tells that the CS not only has intramolecular hydrogen bonding but also intermolecular interactions with TPP during crosslinking. It confirms that the prepared chitosan nanoparticles have high thermal stability than pure CS polymer.

Differential scanning calorimetry

DSC analysis was used to confirm the crystal transformation of the CS-TPP NPs as compared to CS polymer. As clearly indicated in the DSC thermogram, CS-TPP NPs, a broad endothermic peak was observed in 90 – 100 °C range (Fig. 3C). However, CS showed an endothermic low peak at 100 °C that represents the melting temperature of CS (Piyakulawat et al. 2007). For the glass transition temperature (T_g) of CS and CS-TPP NPs was found to be 173.50 °C and 148 – 164 °C range, respectively, thus suggesting the thermal stability of the polymer (Table 2). This confirms that the thermal stability of CS was improved when it is crosslinked with TPP. It could be deduced from these results that the CS with blocked amino groups (for CS-TPP NPs) is thermally less stable than CS with free amino groups.

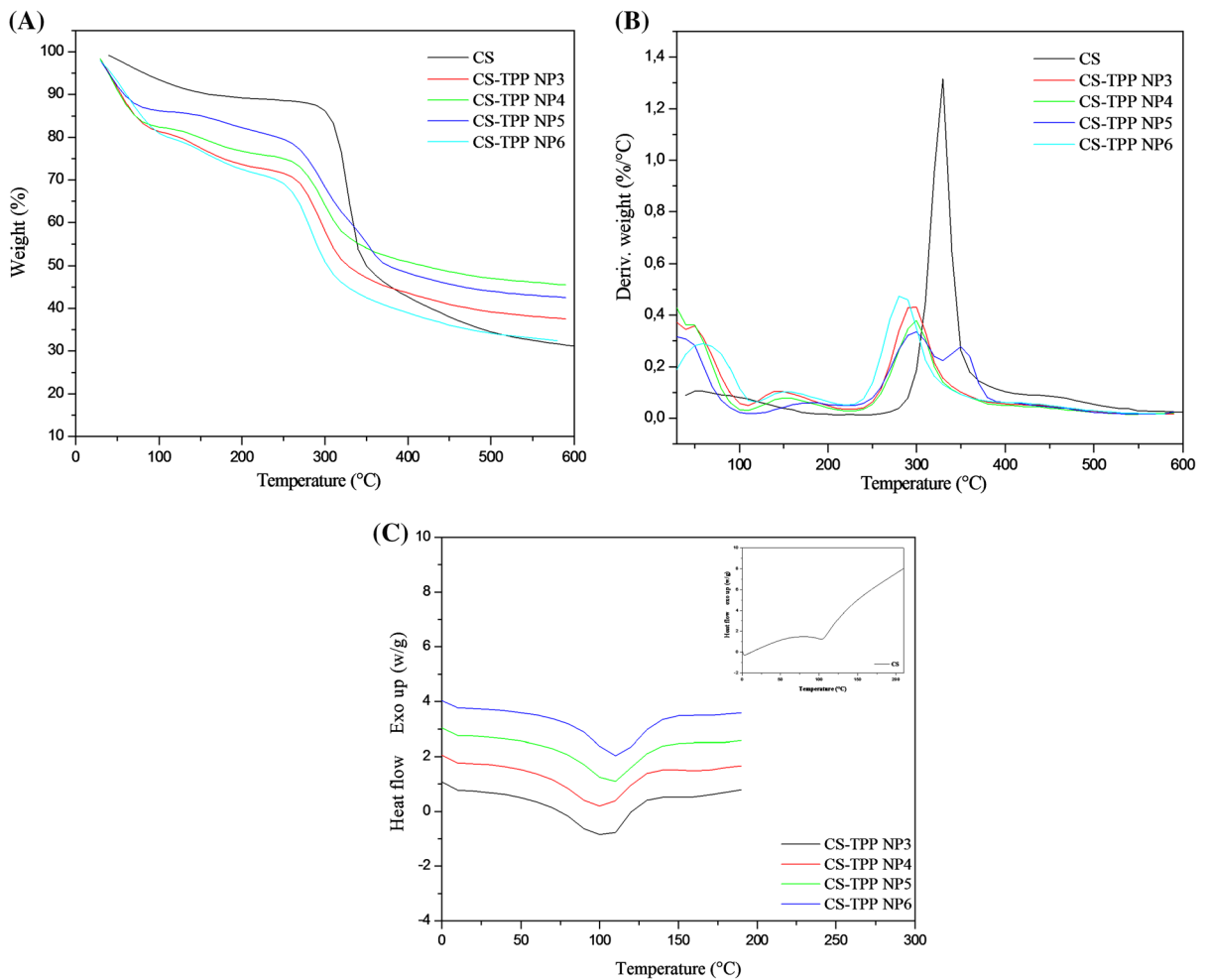


Fig. 3 Thermogravimetric analysis of CS and CS-TPP NPs: curves showing TGA (A) and DTG (B). Thermal stability of CS and CS-TPP NPs by DSC (C)

Table 2 Determination of weight loss percents (ΔW), decomposition temperature (T_d), residual mass and glass transition temperature (T_g) of the prepared CS-TPP NPs

Samples	$\Delta W1$ (%)	$\Delta W2$ (%)	$\Delta W3$ (%)	$\Delta W4$ (%)	T_d (°C)	Residual mass (%)	T_g (°C)
CS	6	62	–	–	329.47	17.50	173.50
CS-TPP NP3	18.91	8.277	29.62	5.63	296.94	37.51	148.43
CS-TPP NP4	17.77	6.38	25.96	4.42	298.30	45.51	151.52
CS-TPP NP5	13.92	4.88	20.67	11.37	297.09	42.45	157.85
CS-TPP NP6	20.35	8.32	32.04	6.77	294.21	32.48	164.77

ΔW : represents the weight losses; T_d : is the decomposition temperature; residual mass: is the residual mass of samples at 600 °C; T_g : is the glass transition temperature

Solubility assessment

One of the key properties of CS and CS-TPP NPs is their solubility. As shown in Table 3, all CS-TPP NPs exhibited a higher solubility ranged from 82.07 to 86.32%. However, CS revealed the highest solubility (95.56%) in 1% acetic acid. Such aqueous and organic solvents solubility could be attributed to the crystalline structure of CS and CS-TPP NPs. Hamdi et al. (2017) reported that CS extracted from blue crab shells was completely soluble in 1% acetic acid.

Water and fat binding capacities

The WBC and FBC of CS and CS-TPP NPs were evaluated for their possible uses as functional ingredients in foods. As shown in Table 3, CS-TPP NPs improved both WBC and FBC since values were significantly higher than those of CS (24.76 and 14.49 g/g of sample), respectively. In addition, results demonstrated that there is a correlation between WBC, FBC and the CS/TPP ratio used for the NPs preparation. Hence, among the prepared NPs, CS-TPP NP6, with CS/TPP ratio of 6/1 and the lowest NPs size (121.6 nm) showed the best ability to bind water (33.18 g/g of sample), while CS-TPP NP5 (153.90 nm) presented the highest FBC (39.07 g/g of sample). In fact, the difference in the water and fat binding capacities could be attributed to the difference in the particles size.

Antioxidant abilities of CS-TPPNPs

To further confirm the antioxidant efficiency of the prepared CS-TPP NPs, four tests were performed such as DPPH radical scavenging activity, ferric

reducing power, β -carotene bleaching-inhibition capacity and ABTS radical scavenging activity.

DPPH radical-scavenging ability

DPPH has an hydrogen free radical and displayed a distinctive absorption at 517 nm. The antioxidants can quench DPPH free radical and convert it into a colorless product, resulting in a decrease in absorbance. In the present study, DPPH radical scavenging capacity of CS-TPP NPs was investigated at different concentrations (1–5 mg/ml), as compared to the CS powder. As shown in Fig. 4A, CS-TPP NPs exhibited notable antioxidant activity against DPPH, in a dose-dependent manner, but still lower than BHA at the same concentration. Further, at 5 mg/ml, CS-TP NP4 exhibited the highest antioxidant activity (74.7%), which is comparable to those obtained for CS at the same concentration (76%).

The half-maximal inhibitory concentration (IC_{50}) values, determined via the regression equation, for the prepared CS-TPP NPs were in the range of 1.7–3.2 mg/ml, against 2.4 mg/ml for pure CS. Therefore, these findings suggest that the amine groups in the CS-TPP NPs could react with free radicals to convert them to more stable molecules and terminate the radical chain reaction by donating protons. Hosseini et al. (2018) reported that fish peptide fraction encapsulated in CS-TPP NPs were characterized by a higher DPPH radical scavenging activity of 75.35% at 5 mg/ml, which is similar to the results of Chi et al. (2015).

β -carotene bleaching-inhibition

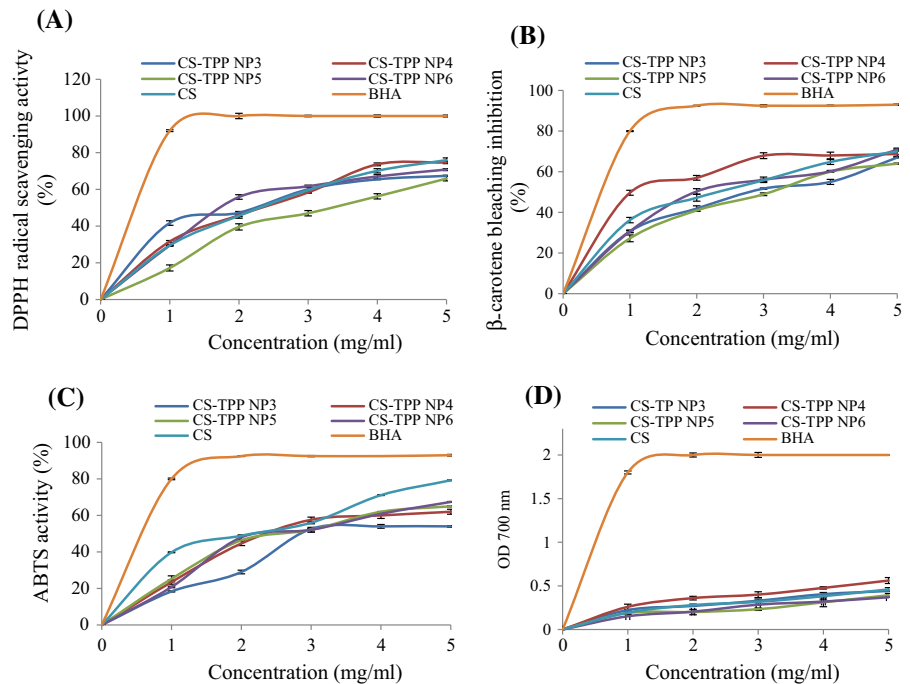
The β -carotene–linoleic bleaching inhibition assay is commonly used for the evaluation of the antioxidant

Table 3 Solubility and functional properties (WBC and FBC) of CS and CS-TPP NPs

Samples	Solubility (%)	WBC (g/g)	FBC (g/g)
CS	95.56 \pm 0.98 ^a	24.76 \pm 0.25 ^c	14.49 \pm 1.43 ^c
CS-TPP NP3	82.07 \pm 0.35 ^c	22.63 \pm 0.37 ^d	27.53 \pm 1.32 ^d
CS-TPP NP4	83.69 \pm 1.06 ^c	26.62 \pm 1.45 ^b	31.17 \pm 0.75 ^c
CS-TPP NP5	86.12 \pm 3.78 ^b	32.08 \pm 0.67 ^a	39.07 \pm 0.23 ^a
CS-TPP NP6	86.32 \pm 1.48 ^b	33.18 \pm 0.62 ^a	33.07 \pm 0.52 ^b

Means with different superscripts (a–d) within a column indicate significant difference ($p < 0.05$)

Fig. 4 Antioxidant potentials of CS and CS-TPP NPs: DPPH-radical scavenging activity (A), β -carotene bleaching inhibition assay (B), ABTS-radical scavenging activity (C) and ferric reducing power assay (D)



activity. In this system founded on oil–water emulsion, in the absence of antioxidants, β -carotene undergoes fast bleaching, which generates free radicals creating peroxy radicals. A free-radical scavenger can inhibit bleaching of β -carotene by neutralizing the linoleate-free radical as well as other free radicals formed during the reaction.

The ability of CS-TPP NPs to protect β -carotene against bleaching as compared to CS was tested. All CS-TPP NPs were able to catch the linoleic hydroperoxyl radicals in a dose-dependent manner (Fig. 4B). In fact, at 5 mg/ml, CS-TPP NP5 and CS-TPP NP6 displayed an important antioxidant activity estimated at about 64% and 71%, respectively, while at the same concentration, the antioxidant activity of CS was about 70%. It can be concluded that CS-TPP NPs could inhibit the β -carotene-bleaching by the neutralization of the linoleate-free radical, as well as others free radicals formed during the reaction. Thus, CS NPs could be used as an antioxidant in food industries.

ABTS radical-scavenging activity

ABTS radical cations decolorization assay is a widely used method for the assessment of the antioxidant

activity of various substances. As observed in Fig. 4C, the antioxidant activity of CS and CS-TPP NPs increased with increasing the concentration of CS NPs. The IC_{50} value of any antioxidant refers to the minimum amount of the substances that is required to scavenge 50% of the radicals generated through the in vitro system. The lowest IC_{50} value was obtained for CS-TPP NP6 (2.3 mg/ml), which was comparable to CS powder (2.1 mg/ml). Nallamuthu et al. (2015) reported a lower IC_{50} value of chlorogenic acid loaded with CS-TPP NPs ($92 \pm 5 \mu\text{g/ml}$).

Reducing power assay

The reducing power ability of the prepared CS-TPP NPs is evaluated at different concentrations ranged from 1 to 5 mg/ml. The results showed a relatively low reducing effect ($OD_{700 \text{ nm}} = 0.4\text{--}0.56$ at 5 mg/ml) (Fig. 4D), in spite of BHA used as reference at the same concentration. These findings were additionally observed for CS ($OD_{700 \text{ nm}} = 0.46$ at 5 mg/ml). Consequently, the prepared CS-TPP NPs and CS were not effective in the reduction of Fe^{3+} to Fe^{2+} by donating electron.

Antimicrobial activity

The damage of foods during the preservation is caused by free radicals, besides the contamination by microbes, which affects the quality of foods and could cause serious health problems to the consumers. The antibacterial activity of the prepared CS-TPP NPs at 10 mg/ml was assessed against two fungal strains and three Gram positive and six Gram negative bacterial strains. It can be concluded that the antibacterial activity depends on the particle size values of CS-TPP NPs (Table 4). In fact, nanoparticles characterized by low particle size values showed the highest bacterial growth inhibition. Among the tested samples, CS-TPP NP6, with lowest nanoparticles size (121.60 nm), showed the highest antimicrobial activity against *B. cereus*, *M. luteus*, *S. enterica* and *Enterobacter* with diameters of inhibition zone in the range of 18–23 mm, which was found to be higher than those of CS. However, TPP powder did not show any antibacterial effect on the different bacteria strains.

In line with Ali et al. (2010), CS-NPs prepared by ionic gelation characterized by a lower particle size (about 100 nm) showed an important antimicrobial activity against *S. aureus* bacteria than that of CS. The authors explained this behavior by a higher specific

area of small particles, and by the fact that at pH 5.5–6.0, the amount of ammonium groups NH_3^+ involved in the nanoparticles formation is lower. It would result in a higher quantity of ammonium groups available for the interactions with the bacterial membranes, which increase the antimicrobial efficiency of NPs. Furthermore, Du et al. (2009) showed that CS-NPs exhibited MIC and MBC values against *E. coli*, *Salmonella choleraesuis*, *Staphylococcus aureus* about 4 times lower compared to CS. However, Qi et al. (2004) estimated the MBC value of CS-NPs 64 times inferior to CS solutions against *E. coli* K88.

The antifungal activity of CS-TPP NPs at 10 mg/ml was evaluated against two pathogenic fungi species (*F. solani* and *R. solani*) by determining the diameter of zone inhibition. As displayed in Table 4, all CS-TPP NPs have high inhibition rates against the tested fungi with inhibition zones between 16 and 19 mm. Interestingly, CS-TPP NPs exhibited a higher antifungal activity against *F. solani* and *R. solani* than CS (15 and 14 mm, respectively) at the same concentration. Results were in accordance with previous studies where the chitosan nanoparticles exhibited higher antimicrobial activity and inhibited 84.72% of *Rhizoctonia solani*, 76.72% of *Collectotrichum acutatum* and 32.16% of *Phytophthora infestans* at 50 mg/ml

Table 4 Antimicrobial activity of CS and CS-TPP NPs against gram-positive and gram-negative bacteria and fungal strains

Bacteria strains	Diameter of inhibition zones (mm)						
	CS-TPP NP3	CS-TPP NP4	CS-TPP NP5	CS-TPP NP6	CS	TPP	Positive control
Gram (+)							
<i>B. cereus</i>	15 ± 0.5	20 ± 1	21 ± 0.4	23 ± 0.25	22 ± 1	ND	20 ± 0.5
<i>S. aureus</i>	17 ± 0.2	16 ± 0.5	18 ± 0.4	17 ± 0.1	21 ± 0.5	ND	25 ± 0.0
<i>M. luteus</i>	10 ± 0.5	16 ± 0.2	18.5 ± 1	20 ± 0.5	13 ± 0.4	ND	19 ± 0.5
Gram (–)							
<i>S. enterica</i>	17 ± 0.1	17.5 ± 0.5	18 ± 0.2	21 ± 0.5	21.5 ± 0.5	ND	20.5 ± 0.5
<i>E. coli</i>	20 ± 1	21 ± 0.5	20.5 ± 0.2	16 ± 0.5	14 ± 1	ND	20 ± 0.5
<i>Enterobacter</i>	10 ± 0.5	12 ± 0.2	15 ± 0.5	18 ± 1	15 ± 1	ND	21 ± 0.2
<i>S. typhimurium</i>	7 ± 0.5	9.5 ± 1	10 ± 0	8 ± 0.1	15 ± 0.3	ND	18 ± 0.5
<i>K. pneumoniae</i>	17 ± 0.5	20 ± 0.2	21 ± 0.5	19 ± 1	15 ± 0.5	ND	12 ± 0.5
<i>P. aeruginosa</i>	11 ± 0.2	12 ± 0.5	16 ± 1	17 ± 0.5	23 ± 0.5	ND	20 ± 1
<i>F. solani</i>	16.5 ± 0.5	19 ± 0.5	17 ± 0.25	19 ± 1	15 ± 0.5	ND	16 ± 0.1
<i>R. solani</i>	17 ± 0.1	16.7 ± 0.3	18.5 ± 0.5	18 ± 0.5	14 ± 0.1	ND	20 ± 0.5

Gram (+): gram positive bacteria; gram (–): gram negative bacteria. ND: not detected. Values were given as mean ± standard deviation. Gentamycine and cycloheximide were used as positive controls for antibacterial and antifungal activities, respectively. Acetic acid solution (0.1%) was used as negative control

and 63.88% of *Fusarium oxysporum* at 40 mg/ml (Divya et al. 2018). The microscopic examination of fungal cultures showed that chitosan nanoparticles disrupt the cell membrane permeability and cause a morphological and molecular alteration of fungal cells. In fact, the exact mechanism of microbial inhibition by CS and CS-TPP NPs still debatable and might be attributed to the amino groups of CS, which promoted the structural disruption of bacterial and fungal cells. In addition, the antimicrobial properties of CS-NPs were also attributed to the small and compact particle size of nanoparticles as well as high surface charge (Qi et al. 2004).

Surimi preservation

Physicochemical properties of surimi

As shown in Fig. 5A, the initial pH values of *surimi* ranged from 6.71 to 6.84 for the three groups (Control, CS and CS-TPP NPs). The pH value of control group showed a decreasing trend during 9 days of storage (pH 6.25), as compared to the CS and CS-TPP NPs groups (pH 6.48 and 6.5). The decrease in pH values could be attributed to the precipitation of alkaline calcium, magnesium and sodium phosphates of the stored *surimi* during the 9 days. It can be concluded that CS and CS-TPP NPs were effective in maintaining the pH values and extending the *surimi* storage.

Furthermore, CS-TPP NPs addition in fish *surimi* formulation prevented the weight loss, increasing therefore the shelf life of the stored *surimi* (Fig. 5B). In fact, the weight loss of *surimi* was at about 10.8 and 6.4% for CS and CS-TPP NPs formulations after 9th day, respectively, compared to that of the control group (19.67%). CS and especially CS-TPP NPs were able to prevent the weight loss by increasing the resistance to water vapor transmission of fish *surimi* during the storage. Previous studies reported that the dense structure of CS makes it a very effective gas barrier (Plainsirichai et al. 2014).

During first day, the process of rehydrating the *surimi* was done properly, as the moisture content of CS and CS-TPP NPs formulations was similar (68–72% range), which was deal for commercial *surimi* production (Fig. 5C). Dey et al. (2013) prepared croaker fish *surimi* and reported a similar result. During the storage, it was observed a remarkable diminution of *surimi* moisture for the control group

(50.9%) on 9th day. However, for the *surimi* incorporated with CS and CS-TPP NPs, there is no difference in the moisture percents (60.2 and 63.1%). Both CS and CS-TPP NPs additives could be effective in maintaining the moisture quantity of *surimi* during 9 days of cold storage. These results were in line with the weight loss of *surimi* during the storage.

Metmyoglobin and myoglobin contents

Metmyoglobin and myoglobin are two main pigments that constitute red color in muscle of fish. In fact, myoglobin concentration generally depends on species, sex and age of animals and the nature of nutrition, oxygen availability and muscle type, as well as the treatment of the meat (Postnikova et al. 1999). For the myoglobin content of fish *surimi*, there is no difference (3.18, 3.02 and 3.33 mg/g) for control, and the treatment with CS and CS-TPP NPs in the first day of storage (Fig. 5D). After 6 days of the cold storage, it was observed a remarkable decrease in the myoglobin content for the control group (2.39 mg/g), as compared to the other treatments (2.68 mg/g for CS and 2.7 mg/g for CS-TPP NPs groups). In fact, previous study reported that the prolonged cold storage reduced the myoglobin contents in sardine and mackerel muscle, which could be attributed to the insolubility of this pigment caused by the myoglobin oxidation to form the metmyoglobin (Chaijan et al. 2005). These changes were due to the intrinsic and extrinsic factors that determinate the metmyoglobin formation. The denaturation and/or oxidation of myoglobin could induce the myoglobin pigment binding with the structural muscle proteins (Ochiai et al. 2001; Chen 2002). Furthermore, Chaijan et al. (2004) showed that the myoglobin contents were higher in the dark muscle than in ordinary muscle of both sardine and mackerel fish. The myoglobin content of frigate mackerel *surimi* was 1.61 and 2.66 times higher than those of Indian mackerel *surimi* and short-bodied mackerel *surimi*, respectively (Chaijan et al. 2010).

The effect of CS and CS-TPP NPs incorporation on the *surimi* metmyoglobin content, during the 9 days of conservation at 4 °C was further investigated. As shown in Fig. 5E, data clearly revealed that there are no significant differences in the metmyoglobin amount (0.41–0.49) at the first day of storage. However, from the 3rd day of cold storage, it was observed a remarkable increase in the metmyoglobin content for

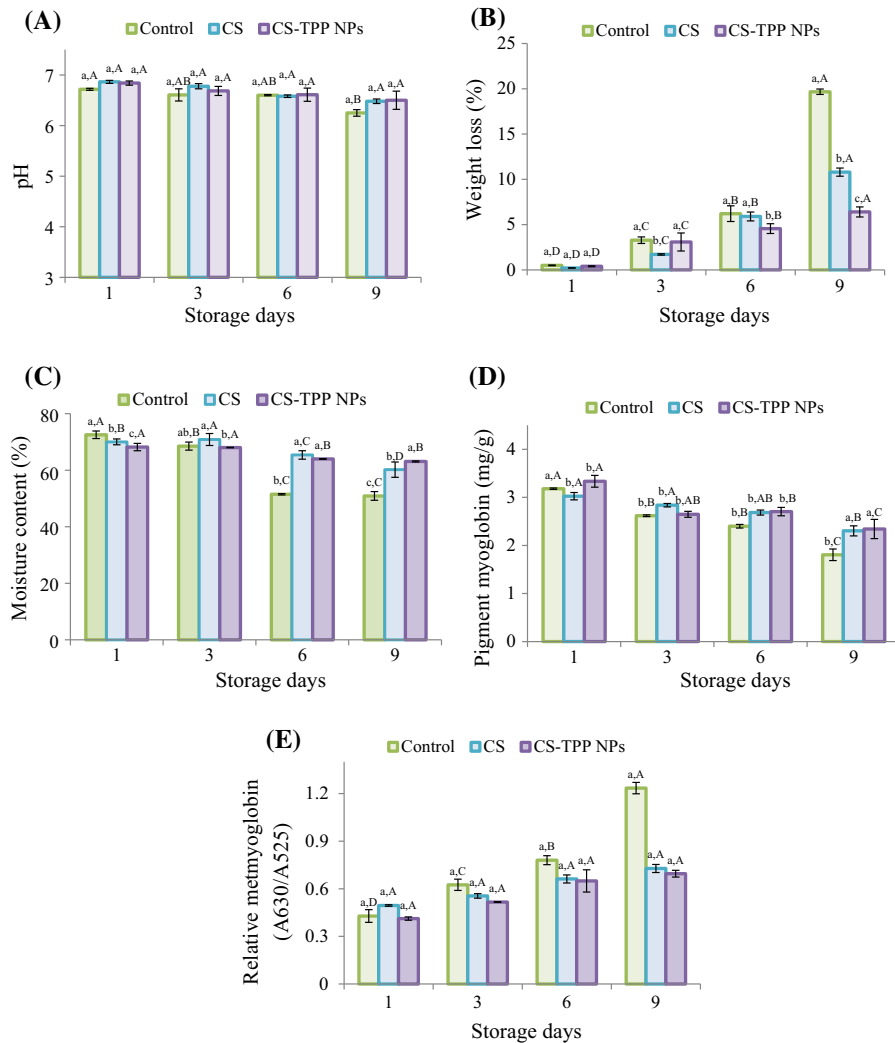


Fig. 5 Determination of pH (A), weight loss (B), moisture content (C), myoglobin (D) and metmyoglobin (E) contents in fish *surimi* samples stored at 4 °C for 9 days. Values with

different letters (a–c) within each parameter in the same day differ significantly ($p < 0.05$). Values with different letters (A–D) in the same treatment differ significantly ($p < 0.05$)

the control group (0.62). For *surimi* supplemented with CS and CS-TPP NPs, a lower oxidation values were obtained with metmyoglobin values of 0.55 and 0.52, respectively. Interestingly, CS and CS-TPP NPs were found to be significantly more efficient in the stabilization and protection of myoglobin pigment than the control formulation. Results were in line with other study, which reported that the total pigments in sardine and mackerel muscles gradually decreased as the storage time increased and suggested that the presence of frigate mackerel and Indian mackerel *surimi* showed a detrimental effect on color of the *surimi* blend (Chaijan et al. 2006).

During the cold storage, an exponential increase of about 1.23 in the metmyoglobin content for the *surimi* without any additive was observed after the 9th day of storage. However, the CS and CS-TPP NPs addition induced a lower increase in the myoglobin oxidation (0.73 and 0.69). Chaijan et al. (2010) showed relative metmyoglobin contents of 0.65 and 0.44 for frigate mackerel and Indian mackerel *surimi*, respectively. Lee et al. (2003) reported that the metmyoglobin formation is positively correlated to the lipid oxidation. During the storage, discoloration of tuna was attributed to the formation of metmyoglobin pigment (Haard 1992).

Lipid oxidation of fish surimi

The MDA, the main secondary product of lipid oxidation, is widely studied as a marker of oxidative stress and lipid peroxidation indices were measured using the TBARS assay. The TBARS values are crucial indicators of the oxidative stability for seafood and derived food products. In fact, the high TBARS values of food products have been correlated with higher rancidity and lower consumer acceptance (Ke et al. 1984). The *surimi* products are highly susceptible to lipid oxidation, which can lead to flavor and color deterioration.

In the present study, the effect of CS and CS-TPP NPs incorporation on lipids oxidation in the *surimi* samples was investigated during 9 days of storage time at 4 °C. The MDA levels determination for the different groups

of *surimi*, depicted in Fig. 6A, show that, independently of the formulation used, the MDA values increased significantly ($p > 0.05$) during the cold storage, but varied among the treatments. It was observed that the control group of *surimi* was the most susceptible to lipid peroxidation with significantly higher MDA values that increase significantly, as a function of storage time, as compared to the other treatments (CS and CS-TPP NPs) in all storage days. Interestingly, CS and especially CS-TPP NPs were found to exhibit an inhibitory role against lipid oxidation of *surimi* during the storage. After 9 days of storage time, control sample showed the highest MDA content (1.42 µg/g of *surimi*), while the *surimi* enriched with CS and CS-TPP NPs exhibited a lower MDA amounts of 0.52 and 0.45 µg/g of *surimi*, respectively.

Ke et al. (1984) proposed that MDA values for seafood products below 0.58 mg/kg are perceived as not rancid, 0.58–1.51 mg/kg slightly rancid, but acceptable, and above 1.51 mg/kg rancid. Using these ranges, *surimi* samples enriched with CS and CS-TPP NPs would be perceived as slightly rancid, but acceptable for the human consumption. Darmadji and Izumimoto (1994) reported that the addition of CS (1%) resulted in a 70% reduction of the TBARS values in beef after storage at 4 °C for 3 days.

The lipid peroxidation of the *surimi* products was equally monitored by the determination of conjugated dienes, which was recognized as the primary oxidation product. As shown in Fig. 6B, the conjugated dienes amounts increased with the storage time for all *surimi* groups, indicating the generation of hydroperoxides substances. For the *surimi* supplemented with CS and CS-TPP NPs, it was observed an increase in conjugated dienes from OD_{233 nm} of 0.24 and 0.28 at 1st day to OD_{233 nm} of 0.56 and 0.45 after 9 days of storage at 4 °C, respectively. However, for the control group, it was observed higher level of conjugated dienes after 9 days of storage time (OD_{233 nm} = 0.7). Therefore, the incorporation of CS and CS-TPP NPs into *surimi* products delayed the oxidation phenomenon, as compared to the control group. These results suggest that both CS-TPP NPs probably contain bioactive agents responsible of the *surimi* protection against lipid peroxidation and able to delay the process of food oxidative degradation. In fact, Shahidi et al. (1999) reported that CS could chelate the free ions, which are released from hemoproteins during heat processing or storage, and thus inhibit the lipid peroxidation of products.

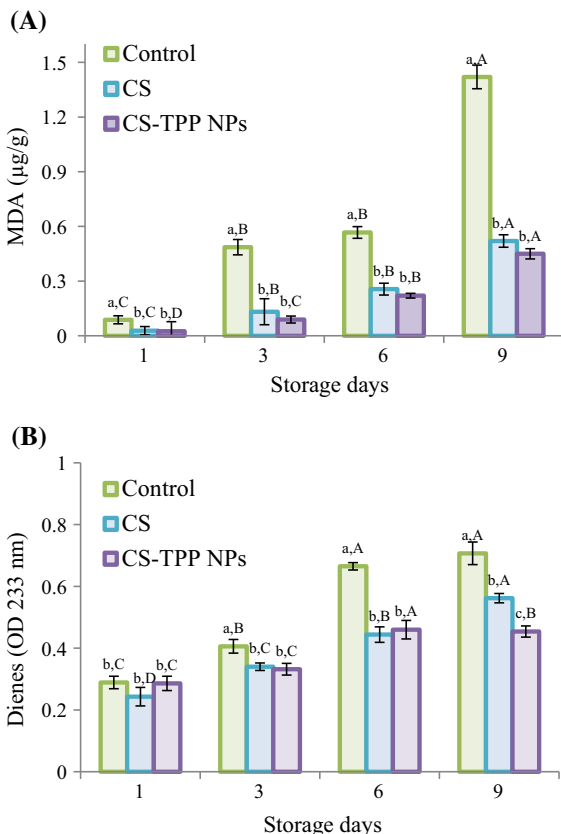


Fig. 6 Effects of CS and CS-TPP NPs incorporation on lipid peroxidation (A) and conjugated dienes (B) of fish *surimi* samples during the cold storage. Values with different letters (a–c) within each parameter in the same day differ significantly ($p < 0.05$). Values with different letters (A–D) in the same treatment differ significantly ($p < 0.05$)

Texture profile analysis

Five factors are determined using texture profile analysis (TPA) of fish *surimi* at the first day and at the end of storage including hardness, springiness, cohesiveness, gumminess and chewiness. Table 5 shows the effects of CS and CS-TPP NPs addition on the texture features of fish *surimi* during storage at 4 °C. Results showed that the texture of samples was not deteriorated during the storage time. However, textural scores for control samples were significantly lower than those of the treated samples. At the first day, there is no significant difference for cohesiveness of the control and *surimi* enriched with CS and CS-TPP NPs groups. During the cold storage, the cohesiveness of the different *surimi* samples was reduced. In fact, the cohesiveness is a measure of the capacity of samples to maintain the interactions and the internal bonds in *surimi* after the first compression cycle of the TPA, thus the cohesiveness value affects the hardness value of *surimi*. At the 9th day, CS and CS-TPP NPs addition gave the highest cohesiveness value than the control groups. The improvement of *surimi* cohesiveness by the CS powder has been as well reported by Rajalekshmi and Mathew (2007) for the threadfin bream *surimi* during the frozen storage.

The *surimi* samples supplemented with CS revealed higher chewiness (24.07 N.mm) ($p < 0.05$) than CS-TPP NPs (16.39 N.mm) and the control (11.54 N.mm) groups at the first day of storage (Table 5). During the storage, the chewiness of the fish *surimi* was significantly reduced. However, the CS-TPP NPs addition improved the chewiness of the samples and was found to be the more effective treatment of *surimi* during the cold storage.

As observed in Table 5, the hardness values exhibited a significant ($p < 0.05$) decrease tendency with *surimi* conservation time. Colmenero et al. (1996) reported that protein contents were responsible for the hardness and were strongly influenced by protein concentration in processed muscle foods. At the end of the storage time, the highest hardness value was obtained for *surimi* enriched with CS (11.01 N) and CS-TPP NPs (11.23 N), compared with that of control group (6.03 N). The high hardness of meat products could be attributed to the reduction of bound water in the batter during the cooking process (Horita et al. 2011). For control samples, the lower hardness values might be related to the proteolytic activity of endogenous or microbial proteases and collagenases (Viji et al. 2014). In the present study, the hardness values of fish *surimi* were much lower than the hardness range of 5181 to 8143 g for fish burgers (Coelho et al. 2007). In fact, Nishimura (2010) reported that the hardness values are commonly associated with the amount of the stromal proteins in fish ranges from 2 to 3%. Further, it has been suggested that the differences in hardness might be further related to the presence of bonds between CS, CS-TPP NPs and myofibrillar proteins via covalent and non-covalent interactions, which improved the texture properties of *surimi* samples (Mao and Wu 2007). In fact, the myofibrillar protein might be affected during the cold storage, which could be translated to the quality of fish *surimi*, as well as the consumer acceptance.

Springiness was defined as the rate at which a deformed *surimi* recovers its initial conditions. The changes in springiness during the cold storage are summarized in Table 5. Results showed that CS and

Table 5 Texture profile analysis (TPA) results for fish *surimi* enriched with CS and CS-TPP NPs after the first and 9th day of chilled storage at 4 °C

Storage days	Samples	Hardness (N)	Adhesiveness (N)	Cohesiveness (ratio)	Chewiness (N.mm)	Springiness (mm)
1	Control	7.33 ± 1.37 ^b	2.94 ± 0.47 ^c	0.35 ± 0.04 ^a	11.54 ± 2.53 ^c	3.70 ± 0.31 ^a
	CS	14.45 ± 2.0 ^a	6.10 ± 0.99 ^a	0.38 ± 0.01 ^a	24.07 ± 2.46 ^a	3.81 ± 0.19 ^a
	CS-TPP NPs	14.52 ± 1.26 ^a	4.32 ± 1.64 ^b	0.35 ± 0.01 ^a	16.39 ± 3.13 ^b	3.38 ± 0.47 ^a
9	Control	6.03 ± 0.39 ^b	2.28 ± 0.4 ^b	0.29 ± 0.01 ^a	7.95 ± 0.54 ^c	3.48 ± 0.22 ^a
	CS	11.01 ± 0.18 ^a	7.51 ± 0.23 ^a	0.37 ± 0.02 ^a	15.64 ± 0.33 ^b	3.67 ± 0.56 ^a
	CS-TPP NPs	11.23 ± 1.09 ^a	2.18 ± 0.75 ^b	0.31 ± 0.01 ^a	17 ± 0.86 ^a	3.86 ± 0.25 ^a

Values with different letters (a, b) within each parameter in the same column differ significantly ($p < 0.05$)

CS-TPP NPs addition didn't show a significant improvement of the springiness values of fish *surimi*. In addition, a low increase in springiness values was detected with the storage time for CS-TPP NPs treatment and attained 3.86 mm at the 9th day. It was observed an increase in adhesiveness values with CS and especially CS-TPP NPs addition onto *surimi* samples. Consequently, the texture of *surimi* samples was not deteriorated during storage time. However, textural scores for control samples were numerically lower than those of treated samples with CS and CS-TPP NPs. Thus, CS-TPP NPs could be used as a natural ingredient to maintain the fish *surimi* based food systems for the development of novel healthy fish products and addresses consumer demands for functional fish products.

Microbial analysis of *surimi*

During storage time, the microbiological quality and shelf life stability of the stored fish *surimi* is commonly recognized. Therefore, the mesophilic, psychrophilic bacteria, yeast and molds plate counts were investigated during the storage time and results are reported in Table 6. The initial mesophilic plate count in the different formulations supplemented with CS and CS-TPP NPs, with respective values of 3.02 and 3 log CFU/g of *surimi*, was similar to that of the control group (3.1 log CFU/g of *surimi*). The mesophilic bacteria counts increased gradually in all samples during storage time. On day 9, CS and CS-

TPP NPs groups attained 5.12 and 4.98 log CFU/g of *surimi*, respectively, which was significantly lower than that of groups without any supplements (control group) reaching 6.45 CFU/g.

Regarding the psychrophilic bacteria plate counts, a rapidly increase from 2.10 to 6.54 log CFU/g of *surimi* after 9 days of storage at 4 °C was observed, as compared to groups supplemented with CS and CS-TPP NPs showing low increase in bacteria growth (Table 6). These results showed that the CS and CS-TPP NPs reduced significantly the mesophilic and psychrophilic bacteria and restricted the growth of microorganisms, which were likewise observed for the yeast and molds plate accounts.

Indeed, on 9th day, *surimi* groups supplemented with CS and CS-TPP NPs had total yeast and molds counts of 4.20 and 4.21 log CFU/g, which was significantly higher for the control group (5.12 log CFU/g). The lower bacterial population is correlated with the higher hardness values of enriched *surimi*, as above mentioned. This could be due to proteinases enzymes that are produced by spoilage microorganisms, which hydrolyze the muscle protein.

Gilbert et al. (2000) reported that a bacteria count of 5 log CFU/g was considered as acceptable limit for restructured products. Based on the microbial analysis results, the fish *surimi* enriched with CS and CS-TPP NPs were in acceptable level for human consumption. However, the control group reached a rejection level after 9 days of storage at 4 °C. This finding was due to the antimicrobial effects of CS and CS-TPP NPs, as

Table 6 Total mesophilic, psychrophilic, yeast and molds plate counts of *surimi* samples at 1, 3, 6 and 9 days of cold storage

Samples		Days of storage			
		1	3	6	9
Mesophilic bacteria	Control	3.1 ± 0.01 ^{a,C}	3.7 ± 0.03 ^{a,BC}	4.2 ± 0.03 ^{a,B}	6.45 ± 0.04 ^{a,A}
	CS	3.02 ± 0.04 ^{b,D}	3.3 ± 0.04 ^{a,C}	4.03 ± 0.07 ^{a,B}	5.12 ± 0.02 ^{b,A}
	CS-TPP NPs	3 ± 0.02 ^{b,D}	3.4 ± 0.06 ^{a,C}	3.9 ± 0.02 ^{a,B}	4.98 ± 0.01 ^{b,A}
Psychrophilic bacteria	Control	2.10 ± 0.01 ^{a,D}	2.8 ± 0.01 ^{a,C}	5.5 ± 0.03 ^{a,B}	6.54 ± 0.01 ^{a,A}
	CS	2.02 ± 0.05 ^{a,D}	2.56 ± 0.02 ^{b,C}	4.87 ± 0.02 ^{b,B}	5.25 ± 0.02 ^{b,A}
	CS-TPP NPs	2.01 ± 0.01 ^{a,C}	2.16 ± 0.04 ^{c,C}	4.7 ± 0.01 ^{b,B}	5.10 ± 0.03 ^{b,A}
Yeast and molds	Control	1.1 ± 0.03 ^{ab,D}	2.34 ± 0.02 ^{a,C}	3.32 ± 0.02 ^{a,B}	5.12 ± 0.01 ^{a,A}
	CS	1.01 ± 0.01 ^{b,D}	2.03 ± 0.04 ^{b,C}	3.18 ± 0.04 ^{a,B}	4.20 ± 0.01 ^{b,A}
	CS-TPP NPs	1.3 ± 0.05 ^{a,D}	2.15 ± 0.03 ^{ab,C}	3.06 ± 0.04 ^{a,B}	4.21 ± 0.02 ^{b,A}

Control: control group; CS: *surimi* enriched with chitosan; CS-TPP NPs: *surimi* enriched with CS-TPP NPs. Values with different letters (a,b) within each parameter in the same column differ significantly ($p < 0.05$)

Values with different letters (A–D) in the same row differ significantly ($p < 0.05$)

previously mentioned. Results were in agreement with those reported by Georgantelis et al. (2007) who found that treatment with CS at a concentration of 0.3–0.6% and 1%, respectively, increased the shelf-life of fresh pork sausages stored at chilled temperature from 7 to 15 days.

Conclusion

CS-TPP NPs with an average size of 121–321 nm were successfully prepared using ionic gelation process. The prepared nanoparticles were characterized by DLS, FTIR, XRD and NMR spectroscopies. Thermogravimetric analysis showed that the CS-TPP NPs were thermally stable, and could be used even at elevated temperatures. CS-TPP NPs were characterized by an interesting antioxidant and antimicrobial activities against Gram-negative and Gram-positive bacteria, as well as fungal strains. As a result, the prepared nanoparticles could be employed in foods and pharmaceutical industries. Further, CS (1%) and CS-TPP NPs (1%) supplements could reduce the microbial growth and the oxidation values of *surimi* samples during 9 days of storage compared to the uncoated one. This suggests that CS-TPP NPs could be a viable solution to maintain the quality of fish *surimi* during the storage. The texture profile analysis parameters were improved by the addition of CS-TPP NPs during the cold storage. Results showed that CS-TPP NPs could be used effectively to extend the shelf life of fish *surimi* products under chilled storage. Thus, CS nanoparticles could be used as a natural ingredient to prevent lipid oxidation in *surimi* based food systems for the development of novel healthy fish products and addresses consumer demands for functional fish products.

Acknowledgments This work was supported by Grants from Ministry of Higher Education and Scientific Research of Tunisia.

References

- Akmaz S, AdJgüzel ED, Yasar M, Erguven O (2013) The effect of Ag content of the chitosan-silver nanoparticle composite material on the structure and antibacterial activity. *Adv Mater Sci Eng*. Article ID 690918, 6
- Ali WS, Joshi M, Rajendran S (2010) Modulation of size, shape and surface charge of chitosan nanoparticles with reference to antimicrobial activity. *Adv Sci Lett* 3:452–460
- Alishahi A, Mirvaghefi A, Tehrani MR, Farahmand H, Shojaosadati SA, Dorkoosh FA, Elsabee MZ (2011) Shelf life and delivery enhancement of vitamin C using chitosan nanoparticles. *Food Chem* 126:935–940
- Anraku M, Fujii T, Furutani N, Kadowaki D, Maruyama T, Otagiri M, Gebicki JM, Tomida H (2009) Antioxidant effects of a dietary supplement: reduction of indices of oxidative stress in normal subjects by water-soluble chitosan. *Food Chem Toxicol* 47:104–109
- Arulmozhi V, Pandian K, Mirunalini S (2013) Ellagic acid encapsulated chitosan nanoparticles for drug delivery system in human oral cancer cell line (KB). *Colloids Surf B* 110:313–320
- Barbi MS, Carvalho FC, Kiill CP, Barud HS, Santagneli SH, Ribeiro SJL, Gremião MPD (2015) Preparation and characterization of chitosan nanoparticles for zidovudine nasal delivery. *Nanosci Nanotechnol* 15:865–874
- Benjakul S, Bauer F (2001) Biochemical and physicochemical changes in catfish muscle as influenced by different freeze-thaw cycles. *Food Chem* 72:207–217
- Bertrand N, Wu J, Xu X, Kamaly N, Farokhad OC (2014) Cancer nanotechnology: the impact of passive and active targeting in the era of modern cancer biology. *Adv Drug Deliv Rev* 66:2–25
- Calero N, Munoz J, Ramirez P, Guerrero A (2010) Flow behaviour, linear viscoelasticity and surface properties of chitosan aqueous solutions. *Food Hydrocoll* 24:659–666
- Calvo P, Remunan Lopez C, Vila Jato JL, Alonso MJ (1997) Novel hydrophilic chitosan-polyethylene oxide nanoparticles as protein carriers. *J Appl Polym Sci* 63:125–132
- Chaijan M, Benjakul S, Visessanguan W, Faustman C (2004) Characteristics and gel properties of muscles from sardine (*Sardinella gibbosa*) and mackerel (*Rastrelliger kanagurta*) caught in Thailand. *Food Res Int* 37:1021–1030
- Chaijan M, Benjakul S, Visessanguan W, Faustman C (2005) Changes of pigments and colour in sardine (*Sardinella gibbosa*) and mackerel (*Rastrelliger kanagurta*) muscle during iced storage. *Food Chem* 93:607–617
- Chaijan M, Benjakul S, Visessanguan W, Faustman C (2006) Changes of lipids in sardine (*Sardinella gibbosa*) muscle during iced storage. *Food Chem* 99:83–91
- Chaijan M, Panpipat W, Benjakul S (2010) Physicochemical properties and gel-forming ability of surimi from three species of mackerel caught in Southern Thailand. *Food Chem* 121:85–92
- Chen HH (2002) Decoloration and gel-forming ability of horse mackerel mince by air-flotation washing. *J Food Sci* 67:2970–2975
- Chi CF, Hu FY, Wang B, Ren XJ, Deng SG, Wu CW (2015) Purification and characterization of three antioxidant peptides from protein hydrolyzate of croceine croaker (*Pseudosciaena crocea*) muscle. *Food Chem* 168:662–667
- Chuah LH, Billa N, Roberts CJ, Burley JC, Manickam S (2011) Curcumin-containing chitosan nanoparticles as a potential mucoadhesive delivery system to the colon. *Pharm Dev Technol* 18:591–599
- Cioffi N, Torsi L, Ditaranto N, Tantillo G, Ghibelli L, Sabbatini L, Bleve-Zacheo T, D'Alessio M, Zambonin PG, Traversa E (2005) Copper nanoparticle/polymer composites with antifungal and bacteriostatic properties. *Chem Mater* 17:5255–5262

- Coelho G, Weschenfelder Â, Meinert E, Amboni R, Beirão LH (2007) Effects of starch properties on textural characteristics of fish burgers: sensory and instrumental approaches. *Boletim Centro de Pesquisa de Processamento de Alimentos* 25:37–50
- Colmenero FJ, Barreto G, Fernández P, Carballo J (1996) Frozen storage of bologna sausages as a function of fat content and of levels of added starch and egg white. *Meat Sci* 42:325–332
- Darmadji P, Izumimoto M (1994) Effect of chitosan in meat preservation. *Meat Sci* 38:243–254
- de Pinho Neves AL, Milioli CC, Müller L, Riella HG, Kuhnen NC, Stulzer HK (2014) Factorial design as tool in chitosan nanoparticles development by ionic gelation technique. *Colloids Surf A Physicochem Eng Asp* 445:34–39
- Dey SS, Dora KC, Raychaudhuri U, Ganguly S (2013) Cryoprotective effect of shrimp waste protein hydrolysate on croaker surimi protein and gel characteristics during frozen storage. *Fish Technol* 50:50–59
- Divya K, Jisha MS (2017) Chitosan nanoparticles preparation and applications. *Environ Chem Lett* 16:101–112
- Divya K, Vijayan S, Jisha MS (2018) Antifungal, antioxidant and cytotoxic activities of chitosan nanoparticles and its use as an edible coating on vegetables. *Int J Biol Macromol* 114:572–577
- Du WL, Niu SS, Xu YL, Xu ZR, Fan CL (2009) Antibacterial activity of chitosan tripolyphosphate nanoparticles loaded with various metal ions. *Carbohydr Polym* 75:385–389
- Dudhani AR, Kosaraju SL (2010) Bioadhesive chitosan nanoparticles: preparation and characterization. *Carbohydr Polym* 81:243–251
- Esterbauer H, Cheeseman KH, Dianzani MU, Poli G, Slater TI (1982) Separation and characterization of the aldehydic products of lipid peroxidation stimulated by ADP Fe^{2+} in rat liver microsomes. *Biochem J* 208:129–140
- Fernandez-Kim SO (2004) Physicochemical and functional properties of crawfish chitosan as affected by different processing protocols. Thesis
- Georgantelis D, Ambrosiadis I, Katikou P, Blekas G, Georgakis SA (2007) Effect of rosemary extract, chitosan and α -tocopherol on microbiological parameters and lipid oxidation of fresh pork sausages stored at 4 °C. *Meat Sci* 76:172–181
- Gilbert RJ, de Louvois J, Donovan T, Little C, Nye K, Ribeiro CD, Richards J, Roberts D, Bolton FJ (2000) Guidelines for the microbiological quality of some ready-to-eat foods sampled at the point of sale. *PHLS advisory committee for food and dairy products. Commun Dis Public Health* 3:163–167
- Gomez-Basauri JV, Regenstein JM (1992) Vacuum packaging, ascorbic acid and frozen storage effects on Heme and Nonheme iron content of Mackerel. *J Food Sci* 57:1337–1339
- Gu HW, Ho PL, Tong E, Wang L, Xu B (2003) Presenting vancomycin on nanoparticles to enhance antimicrobial activities. *Nano Lett* 3:1261–1263
- Haard NF (1992) Biochemistry and chemistry of color and color change in seafoods. *Advances in Seafood Biochemistry*. Technomic Publishing Co, Inc, Lancaster, Penn Sylvania, pp 312–319
- Hajji S, Younes I, Ghorbel-Bellaaj O, Hajji R, Rinaudo M, Nasri M, Jellouli K (2014) Structural differences between chitin and chitosan extracted from three different marine sources. *Int J Biol Macromol* 65:298–306
- Hamdi M, Hajji S, Affes S, Taktak W, Maâlej H, Nasri M, Nasri R (2017) Development of a controlled bioconversion process for the recovery of chitosan from blue crab (*Portunus segnis*) exoskeleton. *Food Hydrocoll* 101:455–463
- Hansen LJ, Sereika HE (1969) Factors affecting color stability of prepackaged frozen fresh beef in display cases. *Illum Eng* 64:620–624
- Hebeish A, Sharaf S, Farouk A (2013) Utilization of chitosan nanoparticles as a green finish in multifunctionalization of cotton textile. *Int J Biol Macromol* 60:10–17
- Horita CN, Morgano MA, Celeghini RMS, Pollonio MAR (2011) Physicochemical and sensory properties of reduced-fat mortadella prepared with blends of calcium, magnesium and potassium chloride as partial substitutes for sodium chloride. *Meat Sci* 89:426–433
- Hosseini SF, Rezaei M, Zandi M, Farahmandghavi F (2015) Fabrication of bio-nanocomposite films based on fish gelatin reinforced with chitosan nanoparticles. *Food Hydrocoll* 44:172–182
- Hosseini SF, Soleimani MR, Nikkiah M (2018) Chitosan/sodium tripolyphosphate nanoparticles as efficient vehicles for antioxidant peptidic fraction from *common kilka*. *Int J Biol Macromol* 111:730–737
- Huang ZM, Zhang Y, Kotaki M, Ramakrishnaj S (2003) A review on polymer nanofibers by electrospinning and their applications in nanocomposites. *Compos Sci Technol* 63:2223–2253
- Jingou J, Shilei H, Weiqi L, Danjun W, Tengfei W, Yi X (2011) Preparation, characterization of hydrophilic and hydrophobic drug in combine loaded chitosan/cyclodextrin nanoparticles and in vitro release study. *Colloids Surf B* 83:103–107
- Jung KH, Lee JH, Park JW, Quach HT, Moon SH, Cho YS, Lee KH (2015) Resveratrol-loaded polymeric nanoparticles suppress glucose metabolism and tumor growth in vitro and *in vivo*. *Int J Pharm* 478:251–257
- Kafshgari MH, Khorram M, Mansouri M, Samimi A, Osfouri S (2012) Preparation of alginate and chitosan nanoparticles using a new reverse micellar system. *Iran Polym J* 21:99–107
- Kanatt SR, Chander R, Sharma A (2008) Chitosan and mint mixture: a new preservative for meat and meat products. *Food Chem* 107:845–852
- Kaya M, Mujtaba M, Ehrlich H, Salaberria AM, Baran T, Amemiya CT, Galli R, Akyuz L, Sargin I, Labidi J (2017) On chemistry of γ -chitin. *Carbohydr Polym* 176:177–186
- Ke PJ, Cervantes E, Robles-Martinez C (1984) Determination of thiobarbituric acid reactive substances (TBARS) in fish tissue by an improved distillation spectrophotometric method. *J Sci Food Agric* 35:1248–1254
- Kim DG, Jeong YI, Choi C, Roh SH, Kang SK, Jang MK, Nah JW (2006) Retinol-encapsulated low molecular water-soluble chitosan nanoparticles. *Int J Pharm* 319:130–138
- Kim IY, Seo SJ, Moon HS, Yoo MK, Park IY, Kim BC, Cho CS (2008) Chitosan and its derivatives for tissue engineering applications. *Biotechnol Adv* 26:1–21
- Kim JH, Kim SI, Kwon IB, Kim MH, Lim JI (2013) Simple fabrication of silver hybridized porous chitosan-based

- patch for transdermal drug-delivery system. *Mater Lett* 95:48–51
- Koleva II, Van Beek TA, Linssen JPH, De Groot A, Evstatieva LN (2002) Screening of plant extracts for antioxidant activity: a comparative study on three testing methods. *Phytochem Anal* 13:8–17
- Lee S, Joo ST, Alderton AL, Hill DW, Faustman C (2003) Oxymyoglobin and lipid oxidation in yellow fin tuna (*Thunnus albacares*) loins. *J Food Sci* 68:1664–1668
- León FJC, Lizardi-Mendoza J, Arguelles-Monal W, Carvajal-Millan E, Lopez Franco YL, Goycoolea FM (2017) Supercritical CO₂ dried chitosan nanoparticles: production and characterization. *RSC Adv* 7:30879–30885
- Li Y, Song H, Xiong S, Tian T, Liu T, Sun Y (2005a) Chitosan-stabilized bovine serum albumin nanoparticles having ability to control the release of NELL-1 protein. *Int J Biol Macromol* 109:672–680
- Li Z, Ramay HR, Hauch KD, Xiao D, Zhang M (2005b) Chitosan-alginate hybrid scaffolds for bone tissue engineering. *Biomaterials* 26:3919–3928
- Maciel VBV, Yoshida CMP, Pereira SMSS, Goycoolea FM, Franco TT (2017) Electrostatic self-assembled chitosan-pectin nano- and microparticles for insulin delivery. *Molecules* 22:1707
- Mao L, Wu T (2007) Gelling properties and lipid oxidation of kamaboko gels from grass carp (*Ctenopharyngodon idellus*) influenced by chitosan. *J Food Eng* 82:128–134
- Meshkini S, Taky AA, Tukmechi A, Farhang-Pajuh F (2012) Effects of chitosan on hematological parameters and stress resistance in rainbow trout (*Oncorhynchus mykiss*). *Vet Res Forum* 3:49–54
- Nallamuthu I, Devi A, Khanum F (2015) Chlorogenic acid loaded chitosan nanoparticles with sustained release property, retained antioxidant activity and enhanced bioavailability. *Asian J Pharm Sci* 10:203–211
- Nguyen TV, Nguyen TTH, Wang SL, Khanh Vo TP, Nguyen AD (2017) Preparation of chitosan nanoparticles by TPP ionic gelation combined with spray drying, and the antibacterial activity of chitosan nanoparticles and a chitosan nanoparticle–amoxicillin complex. *Res Chem Intermed* 43:3527–3537
- Nishimura T (2010) The role of intramuscular connective tissue in meat texture. *Animal Sci J* 81:21–27
- Ochiai Y, Ochiai L, Hashimoto K, Watabe S (2001) Quantitative estimation of dark muscle content in the mackerel meat paste and its products using antisera against myosin light chains. *J Food Sci* 66:1301–1305
- Ocloo FCK, Quayson ET, Adu-Gyamfi A, Quarcoo EA, Asare D, Serfor Armah Y, Woode BK (2011) Physicochemical and functional characteristics of radiation-processed shrimp chitosan. *J Radiat Phys Chem* 80:837–841
- Phromsopha T, Baimark Y (2010) Chitosan microparticles prepared by the water-in-oil emulsion solvent diffusion method for drug delivery. *Biotechnology* 9:61–66
- Piyakulawat P, Praphairaksit N, Chantarasiri N, Muangsing N (2007) Preparation and evaluation of chitosan/carrageenan beads for controlled release of sodium diclofenac. *AAPS Pharm Sci Technol* 8:120–130
- Plainsirichai M, Leelaphatthanapanich S, Wongsachai N (2014) Effect of chitosan on the quality of rose apples (*Syzygium Agueum Alston*) cv. Tabtim Chan stored at an ambient temperature. *APCBEE Proc* 8:317–322
- Postnikova GB, Tselikova SV, Kolaeva SG, Solomonov NG (1999) Myoglobin content in skeletal muscles of hibernating ground squirrels rises in autumn and winter. *Comp Biochem Physiol Part B* 124:35–37
- Qi L, Xu Z, Jiang X, Hu C, Zou X (2004) Preparation and antibacterial activity of chitosan nanoparticles. *Carbohydr Res* 339:2693–2700
- Rajalekshmi M, Mathew PT (2007) Colour and textural parameters of threadfin bream surimi during frozen storage as affected by cryoprotectants and chitosan. *Fish Technol* 44:55–64
- Rodrigues S, Costa AM, Grenha A (2012) Chitosan/carrageenan nanoparticles: effect of cross-linking with tripolyphosphate and charge ratios. *Carbohydr Polym* 89:282–289
- Rokhade AP, Agnihotri SA, Patil SA, Mallikarjuna NN, Kulkarni PV, Aminabhavi TM (2006) Semi-interpenetrating polymer network microspheres of gelatin and sodium carboxymethyl cellulose for controlled release of ketorolac tromethamine. *Carbohydr Polym* 65:243–252
- Ruan S, Yuan M, Zhang L, Hu G, Chen J, Cun X, Gao H (2015) Tumor microenvironment sensitive doxorubicin delivery and release to glioma using angiopep-2 decorated gold nanoparticles. *Biomaterials* 37:425–435
- Shahidi F, Arachchi JKV, Jeon YJ (1999) Food applications of chitin and chitosans. *Trends Food Sci Technol* 10:37–51
- Tokumitsu H, Ichikawa H, Fukumori Y (1999) Chitosan-gadopentetic acid complex. Nanoparticles for gadolinium neutron-capture therapy of cancer: preparation by novel emulsion-droplet coalescence technique and characterization. *Pharm Res* 16:1830–1835
- Vasconcelos F, Cristol S, Paul JF, Tricot GG, Amoureux JP, Montagne L, Mauri F, Delevoeye L (2008) ¹⁷O solid-state NMR and first-principles calculations of sodium trimetaphosphate (Na₃P₃O₉), tripolyphosphate (Na₅P₃O₁₀) and pyrophosphate (Na₄P₂O₇). *Inorg Chem* 47:7327–7337
- Viji P, Tanuja S, Ninan G, Zynudheen AA, Lalitha KV (2014) Quality characteristics and shelf life of sutchi cat fish (*Pangasianodon hypophthalmus*) steaks during refrigerated storage. *Int J Agric Food Sci Technol* 5:105–116
- Wang YF, Huang SR, Shao SH, Qian L, Xu P (2012) Studies on bioactivities of tea (*Camellia sinensis* L.) fruit peel extracts: antioxidant activity and inhibitory potential against α -glucosidase and α -amylase *in vitro*. *Ind Crops Prod* 37:520–526
- Yang HC, Wang WH, Huang KS, Hon MH (2010) Preparation and application of nanochitosan to finishing treatment with anti-microbial and anti-shrinking properties. *Carbohydr Polym* 79:176–179
- Yen GC, Wu J (1999) Antioxidant and radical scavenging properties of extracts from *Ganoderma tsugae*. *Food Chem* 65:375–379
- Yildirim A, Mavi A, Kara AA (2001) Determination of antioxidant and antimicrobial activities of *Rumex crispus* L. extracts. *J Agric Food Chem* 49:4083–4089